Available online at www.sciencedirect.com
ScienceDirect
Journal of Solid State Chemistry 181 (2008) 432–438
JOURNAL OF SOLID STATE CHEMISTRY
www.elsevier.com/locate/jssc

Synthesis and characterization of sulfonated single-walled carbon nanotubes and their performance as solid acid catalyst

Hao Yu, Yuguang Jin, Zhili Li, Feng Peng*, Hongjuan Wang

School of Chemical and Energy Engineering, South China University of Technology, Guangzhou 510641, PR China

Received 12 October 2007; received in revised form 4 December 2007; accepted 16 December 2007
Available online 25 December 2007

Abstract

Single-walled carbon nanotubes (SWCNTs) were treated with sulfuric acid at 300 °C to synthesize sulfonated SWCNTs (s-SWCNTs), which were characterized by electron microscopy, infrared, Raman and X-ray photoelectron spectroscopy, and thermo analysis. Compared with activated carbon, more sulfonic acid groups can be introduced onto the surfaces of SWCNTs. The high degree (~20 wt%) of surface sulfonation led to hydrophilic sidewalls that allows the SWCNTs to be uniformly dispersed in water and organic solvents. The high surface acidity of s-SWCNTs was demonstrated by NH_3 temperature-programmed desorption technique and tested by an acetic acid esterification reaction catalyzed by s-SWCNTs. The results show that the water-dispersive s-SWCNTs are an excellent solid acid catalyst and demonstrate the potential of SWCNTs in catalysis applications.

Keywords: Carbon nanotube; Surface modification; Structural characterization; Raman spectroscopy; Surface reaction

1. Introduction

Since the report of carbon nanotubes (CNTs) by Iijima in 1991 [1], many efforts (see recent review articles [2–4]) have been devoted to the functionalization of CNTs due to the requirement from various applications, including CNT-enhanced composites [5–7], biocompatible materials [8,9], sensors [10–12], optical [13] and catalytic [14,15] materials. Hitherto, a rich variety of methods to modify CNTs have been established, including covalent or noncovalent chemical routes, microwave method [16,17], ionic liquids [18–20], and so on.

The typical functionalization of CNTs is by oxidation [21,22], which introduces oxygen-containing groups, e.g. carboxyl on CNTs, leading to acidic surfaces of CNTs. It has been known that carbon materials are excellent candidates to form solid acid composites [23]. Due to the huge specific surface area of single-walled CNTs (SWCNTs) and their unique surface chemistry, it can be expected that SWCNTs could be used as an effective precursor to synthesize solid acids. The covalent functionalization of CNTs with sulfonic groups provides stability, considerable solubility [16] and strong surface acidity [24]. The sulfonated CNTs are useful for various applications, particularly as solid acid catalysts [24] and excellent catalyst support for highly dispersed metal nanoparticles [25]. So far, the sulfonation of SWCNTs has been achieved by the hydrothermal method [26], microwave-enhanced chemical modification [16] and indirect chemical modification with phenylated SWCNTs [27,28]. The microwave modification is one of the most effective methods to functionalize SWCNTs with carboxylic and sulfonic groups with a ratio about 3:1 [16]. Taking into account the low acidity of carboxylic groups, however, the sulfonation of SWCNTs with high content of sulfonic groups is expected for solid acid applications.

Herein, we report that the functionalization of SWCNTs by concentrated H_2SO_4 at elevated temperatures results in the sulfonation for SWCNTs and tunes the SWCNTs into a hydrophilic material with high acidity. The performance of sulfonated SWCNTs was examined with an esterification reaction as probing reaction and compared with other typical solid acid materials.

*Corresponding author. Fax: +86 20 87114916.
E-mail addresses: yuhao@scut.edu.cn (H. Yu), cefpeng@scut.edu.cn (F. Peng).

0022-4596/$ - see front matter © 2007 Elsevier Inc. All rights reserved.
doi:10.1016/j.jssc.2007.12.017

2. Experimental

2.1. Sulfonation of SWCNTs

SWCNTs used in this work were provided by Tsinghua University [29]. The SWCNTs were first sonicated for 1 h, and then heated at 80 °C for 4 h in the mixture of 1:1 concentrated HNO_3 (65%) and HCl (37%) to remove catalyst particles. These steps also introduced oxygen-containing groups, mainly carboxyl groups on the SWCNTs [21,22,30]. We denoted them as p-SWCNT in the following text. The p-SWCNTs were filtered and washed for times, then dried at 120 °C overnight. Then 50 ml concentrated H_2SO_4 (98%) and 100 mg p-SWCNTs were mixed in a dry flask and then sonicated for 30 min, followed by heating to 250–300 °C (the sulfuric acid boils at 335.5 °C [31]) in an electrothermal heater under dinitrogen atmosphere for 18 h. After the treatment, the suspension was diluted by water and filtered. The solids were washed to remove excess acid and dried at 120 °C to obtain sulfonated SWCNTs (s-SWCNTs). The p-SWCNTs and s-SWCNTs were redispersed in water, ethanol and *N*,*N*-dimethylformamide (DMF) by adding the functionalized SWCNTs into these solvents and then sonicating for 1 h to form 0.5 mg/ml dispersions. For comparison, the sulfonated MWCNTs (s-MWCNTs) and activated carbon (s-AC) were prepared by the same procedure.

2.2. Sample characterizations

The samples were characterized by microscopic and spectroscopic methods, including scanning electron microscopy, transmission electron microscopy, energy dispersive spectrometer (EDS), FTIR, Raman spectroscopy, thermal gravimetric analysis (TGA), and X-ray photoelectron spectroscopy (XPS). SEM images were taken in a LEO 1530VP Microscope equipped with an INCA300 EDS by immobilizing the sample with conductive glue. TEM micrographs were recorded with a JEOL JEM-2010 microscope operated with an acceleration voltage of 200 kV. The samples for TEM were prepared by dispersing CNT samples in anhydrous ethanol to form suspension, then drops of the suspension were loaded on copper grids. The FTIR spectra were recorded with a Bruker 550 spectrometer. The Raman spectra were recorded with a Renishaw RM2000 spectrometer excitated at 785 nm. TGA measurements were performed in a TA Instrument STA449C (Netzsch). XPS spectra were recorded with a Quantum-2000 Scanning ESCA Microprobe with Al$K\alpha$ radiation, calibrated internally by carbon deposit C_{1s}. The surface acidities of functionalized SWCNTs were determined by the ammonia temperature-programmed adsorption–desorption technique (NH_3-TPD) on a TP5000 instrument (Tianjing XianQuan Company). For the NH_3-TPD test, about 20 mg modified SWCNTs were pre-heated at 120 °C to remove adsorbed water. The adsorption was conducted at 35 °C with pulsed NH_3 inputs, and the NH_3 consumption per pulse was detected by a TCD detector.

2.3. Esterification reaction

The acid-catalyzed esterification of acetic acid was employed to evaluate the catalytic activity of modified SWCNTs. The esterification of acetic acid was conducted in liquid phase. For comparison, the experimental conditions were kept the same as that of Ref [32]. In brief, 0.20 g s-SWCNTs were added to a mixture of 0.1 mol acetic acid and 1.0 mol ethanol, and the reaction was carried out at 70 °C in N_2 protection. The liquid products were analyzed by an Agilent 6820 Gas Chromatographer (GC) equipped with capillary columns.

3. Results and discussion

3.1. Microscopic characterizations

The microscopic characterizations by SEM and TEM are shown in Fig. 1. Compared with the pristine SWCNTs, the s-SWCNTs were covered by a layer of foreign matter,

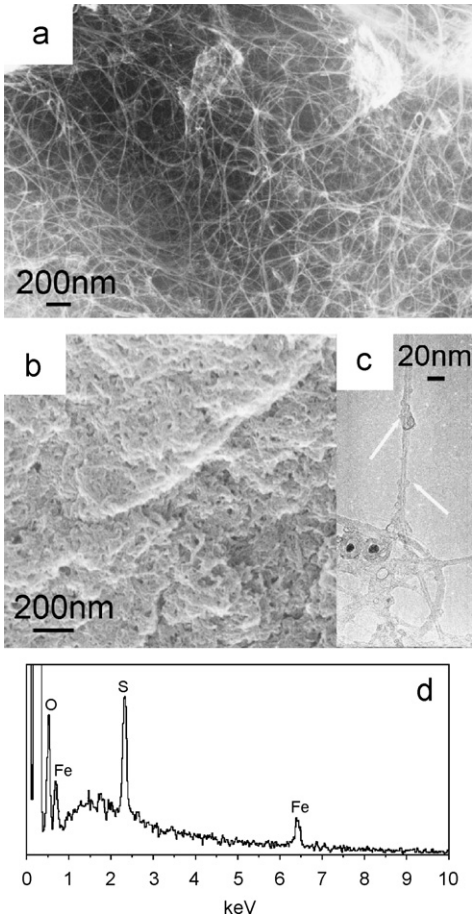

Fig. 1. SEM (a, b) and TEM (c) images of SWCNTs before (a) and after (b, c) the H_2SO_4 treatment. The EDS (d) analysis detected oxygen, sulfur, and iron from residual catalyst. A layer of functional groups on SWCNTs is marked by white arrows in (c).

resulting in thickened SWCNT bundles and a denser network of nanotubes. A microsection element analysis with EDS showed considerable oxygen and sulfur elements, implying the oxygen and sulfur-containing groups. Coating clumps can be observed in the HRTEM of an individual SWCNT exfoliated from a bundle, as marked by the white arrows in Fig. 1(c). These coating materials concentrated in the gaps among nanotubes or their bundles. Taking into account the dramatic morphological change caused by functionalization, it was concluded that the functionalization at high temperature degraded some SWCNTs from the defect sites of p-SWCNTs. The resulting fragments and amorphous carbon attached on the SWCNT scaffold to form a composite structure [33]. The sulfonation can occur on the scaffold as well as the fragments.

3.2. Spectroscopic characterizations

FTIR spectroscopy was employed to investigate the nature of these surface groups. As shown in Fig. 2, the FTIR spectra of p-SWCNTs and s-SWCNTs are compared for the chemical groups on the SWCNTs. FTIR spectrum of p-SWCNTs shows a medium line at 1715 cm^{-1}, which could be assigned to the C═O stretching mode of the –COOH groups. This is a typical feature of oxidized SWCNTs as observed by many groups [16,30,34]. The broad line centered at 3440 cm^{-1} is the contribution from the –OH stretching mode of the –COOH groups. Because the HNO_3 oxidation process introduces not only carboxylic acid, but also alcohol or ketone species, a line at 1170 cm^{-1} from the C–O stretching mode in alcohol species (where the carbon atom is from SWCNT) can be observed. The line at 1630 cm^{-1} was assigned to the C═C stretching mode of SWCNT graphic layers near the modified sites. This mode is weak in perfect SWCNTs due to the symmetry of dipole moment, and will be intensified by defects or holes on graphic layer. The line at 1560 cm^{-1} can be identified with a fundamental mode of SWCNTs [30]. After the H_2SO_4 treatment, the spectrum of s-SWCNTs gave a number of lines. One of the most obvious changes was the enhanced line at 1630 cm^{-1}, which became the strongest line and indicated the extensive functionalization of side walls of SWCNTs. Except for the carboxylic groups (1720 cm^{-1}), the $–SO_2OH$ groups can be identified with the lines at 1317 and 1179 cm^{-1}, representing the SO_2 asymmetric and symmetric stretching modes. When tracer water combines with the sulfonic acid group, these modes shift to 1120 and 1040 cm^{-1}. In low frequency range, the line at 520 cm^{-1} was assigned to C–S stretching mode, suggesting the existence of covalent sulfonic acid groups. The line at 684 cm^{-1} also indicated the S═O stretching mode of $–SO_3H$. The triplet at ~2900 cm^{-1}, responsible for the C–H stretching mode might be resulted from hydrocarbon contamination in spectrometer [30]. It is evident that the H_2SO_4 treatment at high temperature enables the intensive covalent sulfonation of SWCNTs.

The covalent functionalization was also demonstrated by Raman scattering spectroscopy. Fig. 3 shows the Raman spectra of SWCNTs before and after the modifications. All of the Raman spectra were normalized to the G^+ peaks. Compared with the pristine SWCNTs, the D lines of p-SWCNTs and s-SWCNTs significantly increased, indicating the strong damage to the side walls of SWCNTs or the formation of fragments caused by the functionalization. Furthermore, the G^+ line has shifted by ~10 cm^{-1} from 1585 to 1593 cm^{-1} and 1595 cm^{-1}. This is a typical feature of the chemical charge-transfer on oxidized SWCNTs [16,30,35,36]. The existence of radial breathing modes (RBM) in Raman spectra indicated that SWCNTs remained their tubular structure after the functionalization, although some SWCNTs were probably degraded by the strong oxidation. The charge-transfer on the modified SWCNTs also influenced the RBMs. The RBM of raw SWCNTs comprises two major modes, centering at 229

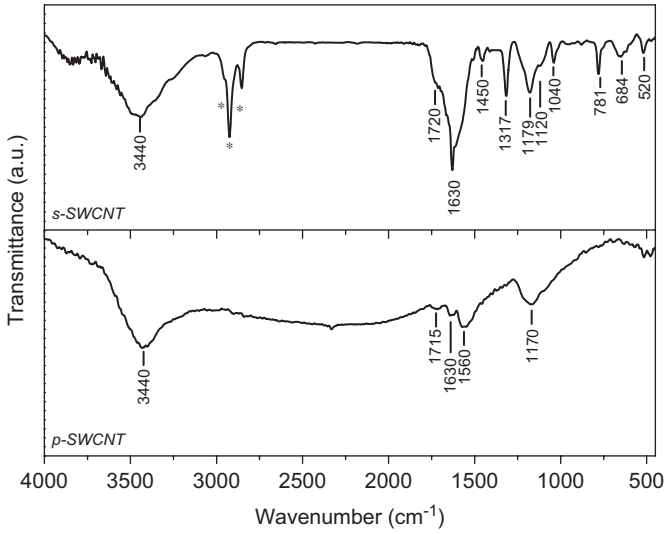

Fig. 2. FTIR spectra of p-SWCNTs and s-SWCNTs.

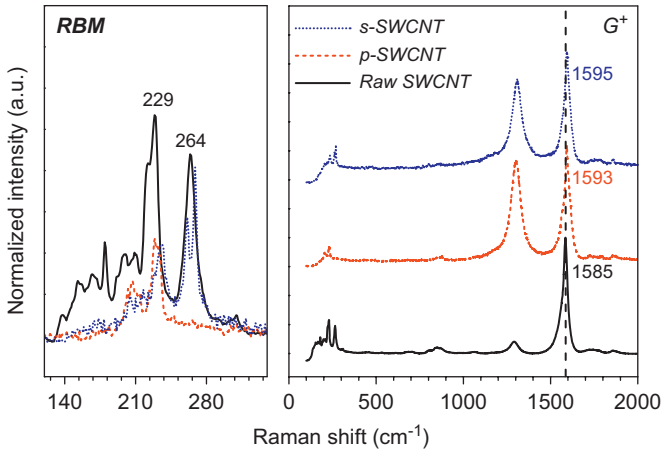

Fig. 3. Raman scattering spectra (excitated at 785 nm and averaged by spectra of three random selected 1 μm spots) of raw SWCNTs, p-SWCNTs, and s-SWCNTs. The intensities have been normalized to the G^+ peaks.

and 264 cm^{-1}, respectively. The line at 264 cm^{-1} was completely quenched in p-SWCNTs, and the one at 229 cm^{-1} was damped in s-SWCNTs. These results are consistent with extensive observations in oxidized SWCNTs, and have been explained by the loss of resonant response due to the shift of Fermi level [37–39]. Above combined spectroscopic characterizations demonstrated that the s-SWCNTs displayed the feature of covalent sulfonation.

XPS was employed to investigate the chemical valences of the surface groups, as shown in Fig. 4. The C_{1s} spectrum can be deconvoluted into three peaks, centered at 284.5, 285.1, and 288.8 eV, respectively. The main peak centered at 284.5 eV originates in sp^2-hybridized graphite carbon. The peak at 285.1 eV is contributed from sp^3-hybridized carbon atoms [40] induced by the strong oxidation of H_2SO_4. The peak at 288.8 eV can be assigned as carbon atoms bound with oxygen or sulfur in functionalized groups, e.g. carboxylic or sulfonic groups [40]. The existence of S was demonstrated by the doublet of S_{2p} peak. The binding energies of $S_{2p1/2}$ at 169.9 eV and $S_{2p3/2}$ at 168.5 eV can be assigned as sulfuric acid or $-SO_2OH$ group [26]. The O_{1s} spectra can be deconvoluted into two peaks. Taking into account the chemical state of oxygen in H_2SO_4 and $-SO_2OH$, the two components in O_{1s} can be assigned as oxygen atoms in S=O and S–OH for the peaks at 533.0 and 531.6 eV, respectively.

3.3. Thermal analysis of s-SWCNTs

The surface groups on SWCNTs were quantitatively investigated by thermogravimetric analysis. The samples were heated from 30 to 900 °C at a ramp rate of 10 °C/min in nitrogen atmosphere. Only 4.2% weight loss was detected for the p-SWCNTs, as shown in Fig. 5. However, distinct weight loss was detected for s-SWCNTs in the range of 200–500 °C. The weight loss over 30% indicated that a large amount of groups were cleaved and decomposed from nanotubes. A parameter study demonstrated that the high temperature is essential for the functionalization. When the SWCNTs were treated at 80 °C, the popular condition for protonation [35,36], a weight loss less than

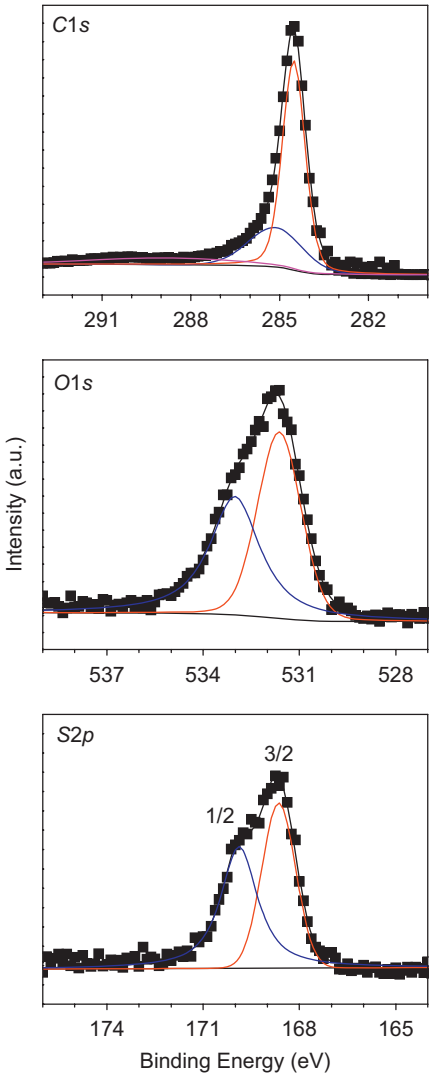

Fig. 4. C_{1s}, O_{1s}, and S_{2p} XPS spectra of s-SWCNTs.

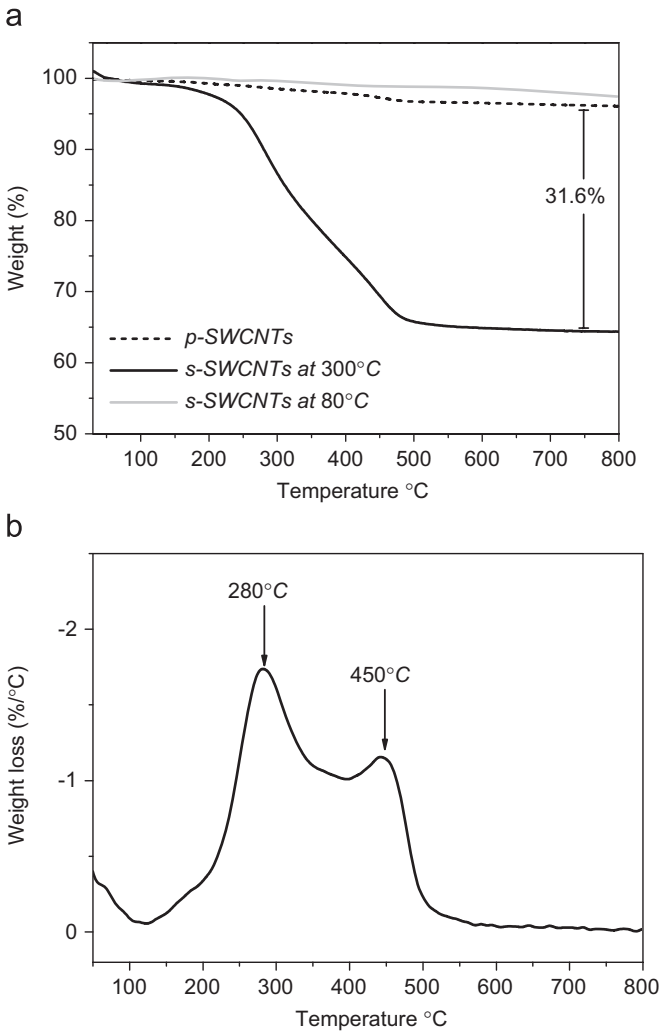

Fig. 5. TG (a) of p-SWCNTs and s-SWCNTs, and DTG (b) of s-SWCNTs.

2% was detected by TG after thorough water-washing. Moreover, the s-SWCNTs treated at 250 °C have weight loss of 19% at 800 °C, indicating that high temperature favors the formation of surface functionality. These results demonstrated that the reaction between SWCNTs and H_2SO_4 behave the different mechanisms at high and low temperatures. To covalently functionalize the relative stable graphitized surface of SWCNTs, high energy has to be provided to overcome the energy barrier for the formation of C–S bond. It should be noted that these groups comprise two components with different thermal stability, as shown in Fig. 5(b). One component decomposes at 280 °C, and the other at 450 °C. We speculated that this was resulted from the intercalation of H_2SO_4 molecular into the groove of SWCNT bundles. They decomposed above 400 °C. As a rough estimation, the weight loss before 400 °C can be attributed to the contribution from cleaving $–SO_2OH$ groups, therefore covalent $–SO_2OH$ groups on the SWCNTs reached 20 wt%, which is equivalent to one covalent $–SO_2OH$ per 24 carbon atoms. It can be reasonably predicted that such a high degree of surface functionalization would bring to SWCNTs hydrophilicity and acidity as solid acids.

3.4. Hydrophilicity and acidity of s-SWCNTs

The compatibility of the functionalized SWCNTs with various solvents was demonstrated by evaluating the dispersibility in water, ethanol, and DMF. The optical photographs of 0.5 mg/ml dispersions of p-SWCNTs and s-SWCNTs are shown in Fig. 6. Although the p-SWCNTs exhibited hydrophilicity to some extent, they precipitated from water and ethanol after standing for days, as shown in the upper panel of Fig. 6. In DMF, a typical polar amide solvent, the p-SWCNTs showed good dispersibility [41,42].

Fig. 6. Optical photographs of dispersions of p-SWCNTs and s-SWCNTs in H_2O, EtOH, and DMF at 0.5 mg/ml.

Table 1
Comparison of surface areas, TG weight losses and acidities of p-SWCNTs, s-SWCNTs, s-MWCNTs and s-AC

Sample	Surface area (m^2/g)	TG weight loss[a] (%)	Acid density[b] (mmol/g)
s-SWCNTs	500	35.6	0.67
p-SWCNTs	500	3.9	0.12
s-MWCNTs[c]	180	15.4	1.90
s-Activated carbon	1200	8.0[d]	0.06

[a]TG weight loss in N_2 at 800 °C.
[b]The acidic site density was defined by the amount of adsorbed NH_3 on the sample.
[c]From Ref. [24].
[d]The TG weight loss of s-AC was calculated by the difference between s-AC and pristine AC, since the strong adsorption of microporous materials led to a significant weight loss of 13.3% on pristine AC.

The dispersibility of SWCNTs was significantly enhanced by sulfonation. The s-SWCNTs dispersed well and formed uniform dispersion in water and ethanol. The solubilities of s-SWCNTs in water, ethanol and DMF were measured as 1.0, 1.3 and 3.0 mg/ml, respectively. These dispersions are stable for even 1 year (the optical photographs in the lower panel of Fig. 6 were taken after 1 year of preparation). Thus, the sulfonation process can be used as an effective method to obtain water-dispersive SWCNTs for a variety of applications, e.g. composites and catalyst supports. Furthermore, the highly sulfonated surfaces of SWCNTs act as a proton carrier; therefore, they can be used as a proton conductor.

The acidity of functionalized SWCNTs has been determined by the NH_3 adsorption technique and shown in Table 1. The sulfonation process endows SWCNTs a high acid density of 0.7 mmol/g. This acid density is about sixfold of p-SWCNTs, which agrees with the TG results and suggests that the s-SWCNTs are a stronger solid acid than p-SWCNTs. It should be noted that, differing from the sulfonated MWCNTs [24], the acidities of functionalized SWCNTs deviated the TG weight losses. We speculated that this deviation was caused by the diffusion limitation in the NH_3-TPD examination, which hindered the detection of acid sites in the grooves of SWCNT bundles and resulted in the underestimation of the acid site density. Nevertheless, the relative rank of acid densities on various samples would not be changed. Compared with the activated carbon (AC), a popular carbon material, SWCNTs exhibited a stronger capability, over 15-fold of sulfonated AC, for acid sites. This result indicates that SWCNTs possess a quite unique surface property to introduce a large amount of $–SO_2OH$ groups. These acid sites make s-SWCNTs act as an effective protonic acid.

3.5. Activity of s-SWCNTs as solid acid

The performance of functionalized SWCNTs, MWCNTs and AC was tested by the esterification of acetic acid and

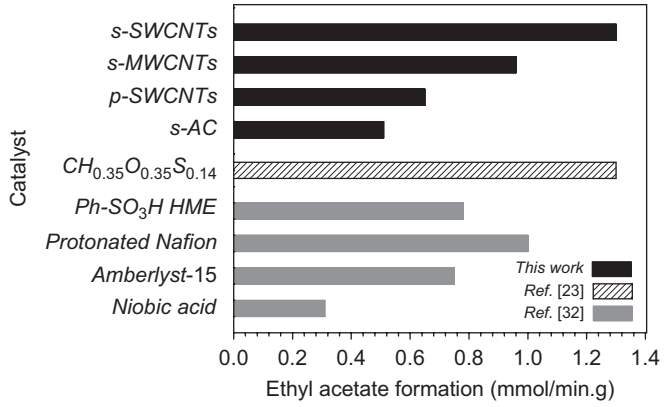

Fig. 7. Catalytic activities of s-SWCNTs, s-MWCNTs, p-SWCNTs, s-AC, and various protonic acids.

compared with some typical solid acid catalysts reported in literatures, as shown in Fig. 7. Five solid protonic acids, including $CH_{0.35}O_{0.35}S_{0.14}$ [23], phenylene-sulfonic acid modified mesoporous ethenylene-silica (Ph-SO_3H HME), protonated Nafion resin, sulfonated polystyrene resin (Amberlyst-15), and niobic acid [32], were selected to make the comparison. The s-SWCNTs showed the higher specific catalytic activity for the esterification reaction to form ethyl acetate than twofold of that of p-SWCNTs and sulfonated AC. This is consistent well with the rank of acidity of these materials and demonstrates the excellent performance of s-SWCNTs as solid acid. Although the intercalation of sulfuric acid reduced the measured value of acid density of s-SWCNTs, s-SWCNTs showed higher activity than s-MWCNTs as expected, due to their large specific surface area. Even compared with one of the best carbon materials as solid acid in literatures [23], s-SWCNTs offered a parallel specific activity. The s-SWCNTs also obviously excelled some typical protonic acid catalysts [32]. Above results demonstrated that the s-SWCNTs created by the high-temperature H_2SO_4 process are highly active as solid acid. The improved activity can be explained by the strong acidity of sulfonic group and, in particular, the ability of SWCNTs to support functional groups. Another reason responsible for the enhanced catalytic performance is the excellent dispersibility in solvents, including ethanol, which minimizes the mass transfer resistance in the heterogenous liquid–solids reaction.

4. Conclusions

Sulfonated SWCNTs were prepared by a high-temperature H_2SO_4 process. By treating the SWCNTs with concentrated sulfuric acid at 300 °C, covalent $-SO_2OH$ groups were created on the surface of SWCNTs. In this process, about 20 wt% $-SO_2OH$ groups are supported on SWCNTs, which transforms the hydrophobic surface of pristine SWCNTs to a hydrophilic surface. Resulting functionalized SWCNTs can be stably dispersed in water. Compared with activated carbon and MWCNTs, more sulfonic acid groups can be introduced onto the surfaces of SWCNTs. Due to the strong acidity of surface sulfonic acid groups, the functionalized SWCNTs provide an excellent performance as solid acid catalyst. Thus, the method in this paper provides a novel and potential nanomaterials as an efficient solid acid catalyst, and demonstrates the potential of SWCNTs in the catalysis field.

Acknowledgments

We thank Profs. Zhou Jian and Zhang Lei in School of Chemical and Energy Engineering, South China University of Technology, for their helpful discussions. We thank the Beijing Key Laboratory of Green Reaction Engineering and Technology in Tsinghua University for the convenience of using high-resolution transmission electron microscope. This work was supported by the Guangdong Provincial Science and Technology Project (no. 2006A10903002) and Guangzhou Civic Science and Technology Project (no. 2007Z3-D2101).

References

[1] S. Iijima, Nature 354 (1991) 56–58.
[2] D.A. Britz, A.N. Khlobystov, Chem. Soc. Rev. 35 (2006) 637–659.
[3] S. Banerjee, T. Hemraj-Benny, S.S. Wong, Adv. Mater. 17 (2005) 17–29.
[4] D. Tasis, N. Tagmatarchis, A. Bianco, M. Prato, Chem. Rev. 106 (2006) 1105–1136.
[5] J.N. Coleman, U. Khan, W.J. Blau, Y.K. Gun'ko, Carbon 44 (2006) 1624–1652.
[6] J.N. Coleman, U. Khan, Y.K. Gun'ko, Adv. Mater. 18 (2006) 689–706.
[7] X.L. Xie, Y.W. Mai, X.P. Zhou, Mater. Sci. Eng. R-Rep. 49 (2005) 89–112.
[8] S. Polizu, O. Savadogo, P. Poulin, L. Yahia, J. Nanosci. Nanotechnol. 6 (2006) 1883–1904.
[9] Y. Lin, S. Taylor, H.P. Li, K.A.S. Fernando, L.W. Qu, W. Wang, L.R. Gu, B. Zhou, Y.P. Sun, J. Mater. Chem. 14 (2004) 527–541.
[10] S.E. Moulton, A.I. Minett, G.G. Wallace, Sens. Lett. 3 (2005) 183–193.
[11] K.P. Gong, Y.M. Yan, M.N. Zhang, L. Su, S.X. Xiong, L.Q. Mao, Anal. Sci. 21 (2005) 1383–1393.
[12] Q. Zhao, Z.H. Gan, Q.K. Zhuang, Electroanalysis 14 (2002) 1609–1613.
[13] J.J. Zhao, X.S. Chen, J.R.H. Xie, Anal. Chim. Acta 568 (2006) 161–170.
[14] G.G. Wildgoose, C.E. Banks, R.G. Compton, Small 2 (2006) 182–193.
[15] P. Serp, M. Corrias, P. Kalck, Appl. Catal. A-Gen. 253 (2003) 337–358.
[16] Y.B. Wang, Z. Iqbal, S. Mitra, J. Am. Chem. Soc. 128 (2006) 95–99.
[17] Y.B. Wang, Z. Iqbal, S. Mitra, Carbon 43 (2005) 1015–1020.
[18] M.J. Park, J.K. Lee, B.S. Lee, Y.W. Lee, I.S. Choi, S.G. Lee, Chem. Mater. 18 (2006) 1546–1551.
[19] B.K. Price, J.L. Hudson, J.M. Tour, J. Am. Chem. Soc. 127 (2005) 14867–14870.
[20] S. Bellayer, J.W. Gilman, N. Eidelman, S. Bourbigot, X. Flambard, D.M. Fox, H.C. De Long, P.C. Trulove, Adv. Funct. Mater. 15 (2005) 910–916.
[21] T.W. Ebbesen, P.M. Ajayan, H. Hiura, K. Tanigaki, Nature 367 (1994) 519.

[22] H. Hiura, T.W. Ebbesen, K. Tanigaki, Adv. Mater. 7 (1995) 275–276.
[23] M. Hara, T. Yoshida, A. Takagaki, T. Takata, J.N. Kondo, S. Hayashi, K. Domen, Angew. Chem. Int. Ed. 43 (2004) 2955–2958.
[24] F. Peng, L. Zhang, H.J. Wang, P. Lv, H. Yu, Carbon 43 (2005) 2405–2408.
[25] H.J. Wang, H. Yu, F. Peng, P. Lv, Electrochem. Commun. 8 (2006) 499–504.
[26] G.S. Duesberg, R. Graupner, P. Downes, A. Minett, L. Ley, S. Roth, N. Nicoloso, Synth. Met. 142 (2004) 263–266.
[27] F. Liang, J.M. Beach, P.K. Rai, W.H. Guo, R.H. Hauge, M. Pasquali, R.E. Smalley, W.E. Billups, Chem. Mater. 18 (2006) 1520–1524.
[28] B. Yi, R. Rajagopalan, H.C. Foley, U.J. Kim, X.M. Liu, P.C. Eklund, J. Am. Chem. Soc. 128 (2006) 11307–11313.
[29] G.Q. Ning, F. Wei, Q. Wen, G.H. Luo, Y. Wang, Y. Jin, J. Phys. Chem. B 110 (2006) 1201–1205.
[30] U.J. Kim, C.A. Furtado, X.M. Liu, G.G. Chen, P.C. Eklund, J. Am. Chem. Soc. 127 (2005) 15437–15445.
[31] J.A. Dean, Lange's Handbook of Chemistry, McGraw-Hill, New York, 1999, p. 3.33.
[32] K. Nakajima, I. Tomita, M. Hara, S. Hayashi, K. Domen, J.N. Kondo, Adv. Mater. 17 (2005) 1839–1842.
[33] C.G. Salzmann, S.A. Llewellyn, G. Tobias, M.A.H. Ward, Y. Huh, M.L.H. Green, Adv. Mater. 19 (2007) 883–887.
[34] J. Zhang, H.L. Zou, Q. Qing, Y.L. Yang, Q.W. Li, Z.F. Liu, X.Y. Guo, Z.L. Du, J. Phys. Chem. B 107 (2003) 3712–3718.
[35] S. Ramesh, L.M. Ericson, V.A. Davis, R.K. Saini, C. Kittrell, M. Pasquali, W.E. Billups, W.W. Adams, R.H. Hauge, R.E. Smalley, J. Phys. Chem. B 108 (2004) 8794–8798.
[36] C. Engtrakul, M.F. Davis, T. Gennett, A.C. Dillon, K.M. Jones, M.J. Heben, J. Am. Chem. Soc. 127 (2005) 17548–17555.
[37] M.S. Strano, C.B. Huffman, V.C. Moore, M.J. O'Connell, E.H. Haroz, J. Hubbard, M. Miller, K. Rialon, C. Kittrell, S. Ramesh, R.H. Hauge, R.E. Smalley, J. Phys. Chem. B 107 (2003) 6979–6985.
[38] W. Zhou, J. Vavro, N.M. Nemes, J.E. Fischer, F. Borondics, K. Kamaras, D.B. Tanner, Phys. Rev. B 71 (2005) 205–423.
[39] X.F. Zhang, T.V. Sreekumar, T. Liu, S. Kumar, J. Phys. Chem. B 108 (2004) 16435–16440.
[40] H. Ago, T. Kugler, F. Cacialli, W.R. Salaneck, M.S.P. Shaffer, A.H. Windle, R.H. Friend, J. Phys. Chem. B 103 (1999) 8116–8121.
[41] C.A. Furtado, U.J. Kim, H.R. Gutierrez, L. Pan, E.C. Dickey, P.C. Eklund, J. Am. Chem. Soc. 126 (2004) 6095–6105.
[42] J.L. Bahr, E.T. Mickelson, M.J. Bronikowski, R.E. Smalley, J.M. Tour, Chem. Commun. (2001) 193–194.